Multiple Shape Memory Behavior of Highly Oriented Long-chain-branched Poly(lactic acid) and Its Recovery Mechanism

[1]Jiafeng Li, [1]Xiaowen Zhao, [1]Lin Ye*, [2]Phil Coates, [2]Fin Caton-Rose

1. State Key Laboratory of Polymer Materials Engineering of China, Polymer Research Institute of Sichuan University, Chengdu, China

2. School of Engineering, Design and Technology, University of Bradford, Bradford, U.K.

*Corresponding author. Tel.: 862885408802; Fax: 862885402465. E-mail address: yelinwh@126.com

Abstract: The shape memory effect of highly oriented long-chain-branched Poly(lactic acid) (LCB-PLA) prepared through solid-phase die drawing technology was studied by comparison with PLA. When the recovery temperature increased form 60 $^\circ$C to 120 $^\circ$C, for PLA, only one-step recovery at about 80°C can be observed and the recovery ratio was below 21.5%, while, for LCB-PLA, multiple recovery behavior with high recovery ratio of 78.8% can be achieved. For oriented PLA, the recovery curve of the final sample showed the same trend with that of sample suffering just free drawing; while for oriented LCB-PLA, the recovery curve of the final sample showed the same trend with that of sample suffering just die drawing. After shape recovery, the mechanical properties of LCB-PLA showed a linear downward trend with the recovery temperature. Together with amorphous phase, the oriented mesomorphic phase, which formed during solid die drawing, can act as switching domains. And thus, upon heating, the chain segment of amorphous phase relaxed at first and triggered the first macroscopical shape recovery, leading to the decrease of long period (L_{ac}) and the thickness of the amorphous layer (L_a). Then, with further increasing temperature, the oriented mesomorphic phase gradually relaxed resulting subsequently multi-shape recovery, and the L_{ac} and the L_a further decreased. Therefore, by regulating the recovery temperature of oriented LCB-PLA, the shape recovery ratio and mechanical strength can be controlled effectively, and thus the self-reinforced and self-fastening effect can be achieved simultaneously for PLA as bone fixation material.

Keywords: Long-chain-branched poly (lactic acid) (LCB-PLA); Solid-phase die drawing; Multiple shape memory behavior; Recovery mechanism

INTRODUCTION

Poly (lactic acid) (PLA, $-[CH(CH_3)COO]_n-$) was recognized as a very promising substitute for biomedical materials because of its nontoxic nature, biocompatibility and biodegradability, and approved for use in a number of clinical applications by Food and Drug Administration (FDA) [1~5]. The development of high strength PLA materials as absorbable bone fixation devices started in the 1970s. Compared with conventional metallic and ceramic bone fixation materials, the superior biomechanical properties and appropriate degradation rate of PLA made it to be a promising alternative for temporary bone fracture, which can decrease morbidity of the surgical complications by avoiding stress shielding and the necessity of a second operation [6~7]. However, some properties of PLA were far less than expected when it acts as implanted bone fixation materials: the mechanical strength of non-reinforced PLA for fixation of weight loading bones is not sufficient; some intelligent functionality such as self-fastening property is deficient compared with some shape memory alloy.

Molecular orientation could significantly enhance the mechanical properties of PLA. Long Y et al. prepared amorphous and semi-crystalline PLA films with oriented structure through die extrusion [8]. The tensile strength and modulus at a draw ratio of 200% could be more than 121 MPa and 3.8 GPa, respectively. Yuan et al. prepared PLLA fibers via the melt-spinning method, and the tensile modulus of 3.6~5.4 GPa was achieved at the draw ratio of 589% [9]. By using the method of dry-jet-wet spinning, Bhuvanesh Gupta et al. also prepared PLA fibers, showing that the draw ratio could reach the maximum of 1000% and the draw ratio showed important influence on its structural development [10]. In our previous study, for the purpose of overcoming the great difficulty in ultra-drawing of PLA due to its very low melt strength, thereby obtaining high degree of orientation, through reactive processing,

long-chain-branched PLA (LCB-PLA) was prepared [11]. Very high draw ratio about 1200% can be achieved for LCB-PLA, and for the oriented sample, the tensile modulus and strength can reach up to 7.2 GPa and 228 MPa, respectively, which basically satisfied its application as born fixation materials [12].

As a kind of semi-crystalline polymer, for both PLA and LCB-PLA, their crystalline domains and molecular entanglement can serve as the fixed phase, while their amorphous domains can act as the reversible phase to realize thermally induced shape memory effect to a certain extent, and thus self-fastening function can be achieved for PLA to be used as implant bone fixation screw. However, literatures, which explained the shape memory behavior of PLA influenced by orientation, could be hardly available.

Solid die drawing technology is one of the convenient methods for molecular orientation of polymers in solid state. Compared with other orientation processes, such as free solid drawing [13, 14] and electrospinning [15, 16], through solid die drawing process, not only high production rates and high orientation can be achieved without using complex processing apparatus, but thick section samples including tubes, tapes, etc. can also be produced [17, 18]. Die drawing process can be divided into two stages, including die drawing stage, during which samples are axially deformed within the die, and free drawing stage, during which samples undergo free drawing out of the die exit and further axial extension occurs. Because quite different structure formed for PLA samples with different entanglement during the above mentioned two stages of solid die drawing, it's necessary to study the effect of the two stages of solid die drawing on the recovery ratio of samples to obtain better understanding on the shape recovery behavior of oriented samples produced through this technology.

In this work, highly oriented PLA and LCB-PLA samples were obtained via the technology of solid die drawing. The influence of recovery temperature and different stages of solid die drawing process on the shape memory behavior of the highly oriented samples was studied. The evolution of the oriented crystalline structure during orientation process and shape recovery process was explored for both PLA and LCB-PLA, and thus the recovery mechanism was revealed, aiming to simultaneously realize self-enhancement and self-fastening effect through adjusting the recovery temperature and shape recovery ratio when acted as bone fixation material.

MATERIALS AND METHODS

Materials

Poly (lactic acid) (PLA) was purchased from Nature Works Co., USA, while the molecular weight (M_w) was about 1×10^5 and the molecular weight distribution index (M_w/M_n) was about 1.21. Pyromellitic dianhydride and Pentaerythritol polyglycidyl ether were supplied by Sinopharm Chemical Reagent Company and Energy Chemical Reagent Company, respectively.

Orientation of PLA and LCB-PLA samples

LCB-PLA samples were obtained based on our previous work [9]. Orientation of PLA and LCB-PLA samples was performed on a die-drawing apparatus. Firstly, PLA and LCB-PLA billets were preheated for 3~15 min at 60~100°C, and then they were drawn through the die.

Measurements

Shape memory behavior

By putting oriented PLA samples in the thermostatic oil bath with temperature of 60, 80, 100 and 120°C, respectively, for 30 min, the shape recovery behavior of highly oriented PLA samples was examined. The shape recovery ratio (R_r) of the samples

could be calculated as follow [19]:

$$R_r=(L_1-L_2)/(L_1-L_0) \qquad (1)$$

where，L_0 was the sample length before deformation; L_1 was the sample length after deformation; L_2 was the sample length after recovery.

Dynamic mechanical analysis (DMA)

Dynamic mechanical analyses of PLA samples were conducted on the DMA Q-800 (TA Instruments, USA) to further characterize their one-way shape recovery behavior under a controlled force actuator mode. The heating rates were 10°C/min. Recovery ratio (R_ε) can be calculated as below [20]:

$$R_\varepsilon=(\varepsilon-\varepsilon_{rec})/\varepsilon \bullet 100\% \qquad (2)$$

where, ε and ε_{rec} were the strains before and after recovery, respectively.

Two-dimensional wide-angle X-ray diffraction (2D-WAXD) analysis

2D-WAXD analysis of PLA samples was performed on the D8 Discover 2D-WAXD (Bruker AXS Co., Germany) at the ambient temperature.

## Two-dimensional small-angle X-ray scattering (2D-SAXS) analysis

2D-SAXS analysis of PLA samples was conducted by using the Synchrotron Radiation Facility (Shanghai) with a beam line of BL16B1 (λ= 1.24A).

RESULTS

The effect of recovery temperature on the shape memory behavior of oriented PLA and LCB-PLA

Photos of highly oriented PLA and LCB-PLA samples after recovery at different temperature were shown in Fig.1. Obviously, the lengths of the two kinds of samples before recovery were 11.5~11.8mm. After samples being recovered at 60°C, the sample lengths remained almost constant for both samples. With increasing recovery

temperature from 60 $^{\circ}$C to 120 $^{\circ}$C, for PLA, only one clear recovery of the sample length from 11.5 mm to 10.6 mm can be observed at about 80°C, and the R_r was about 12%. While for LCB-PLA, an obvious recovery of the sample length from 11.8 mm to 10.5 mm can also be observed at 80 $^{\circ}$C, moreover, when the recovery temperature further increased to 100~120 $^{\circ}$C, the sample lengths presented to recover further from 10.5 mm to 8.8~5.4 mm, and the R_r can reached about 85.5% at 120 $^{\circ}$C. Therefore, it can be concluded that, during this whole process, multiple recovery behavior with high R_r can be achieved for oriented LCB-PLA sample.
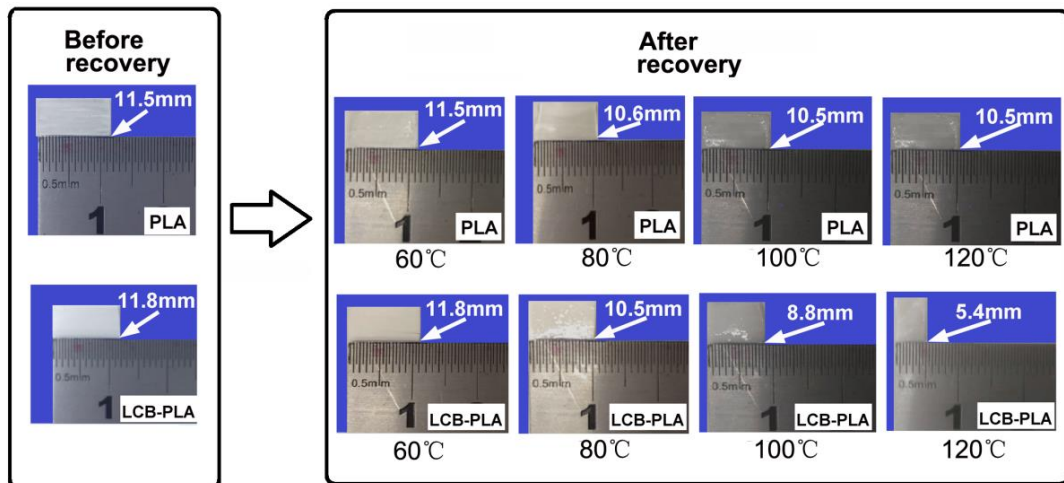
Fig. 1 Photos of shape recovery process for oriented PLA and LCB-PLA after recovery at different temperature

In order to further explore the shape recovery behavior of highly oriented PLA as bone fixation materials, DMA measurement was conducted and an intermittently heating procedure was made for the test. During this procedure, oriented PLA samples were quickly heated to 40, 60, 80, 100, 120°C and maintained at each temperature for about 15 minutes to make sure that samples recovered their shape completely. As shown in Fig.2(a~b), it can be seen that, when the recovery temperature was below 60 $^{\circ}$C, the recovery ratio (R_ε) was very low for both oriented PLA and LCB-PLA samples, which may be attributed to that the glassy state hindered the movement of PLA chains at low temperature ($<T_g$). When samples were heated to 80 $^{\circ}$C, the R_ε of

21.5% was achieved for PLA, and thereafter, with the continuous increase of recovery temperature from 80 ℃ to 120 ℃, the R_ε of PLA samples maintained constant instead of increasing continually, indicating the one-step recovery at 80°C. While, for oriented LCB-PLA samples, R_ε reached 22.7% at 80 ℃, and then that value increased respectively to 43.6% at 100 ℃ and 78.8% at 120 ℃, suggesting the obvious multiple shape recovery behavior.

The recovery stress of oriented samples during recovery was shown in Fig.2(c). When the recovery temperature was below 80° C, for both PLA and LCB-PLA, the recovery stress increased sharply with temperature. However, when the temperature further increased, for PLA, the recovery stress decreased obviously, while for LCB-PLA, it remained at a relatively high value, suggesting the high driving force for shape recovery in the range of 60~120 °C.
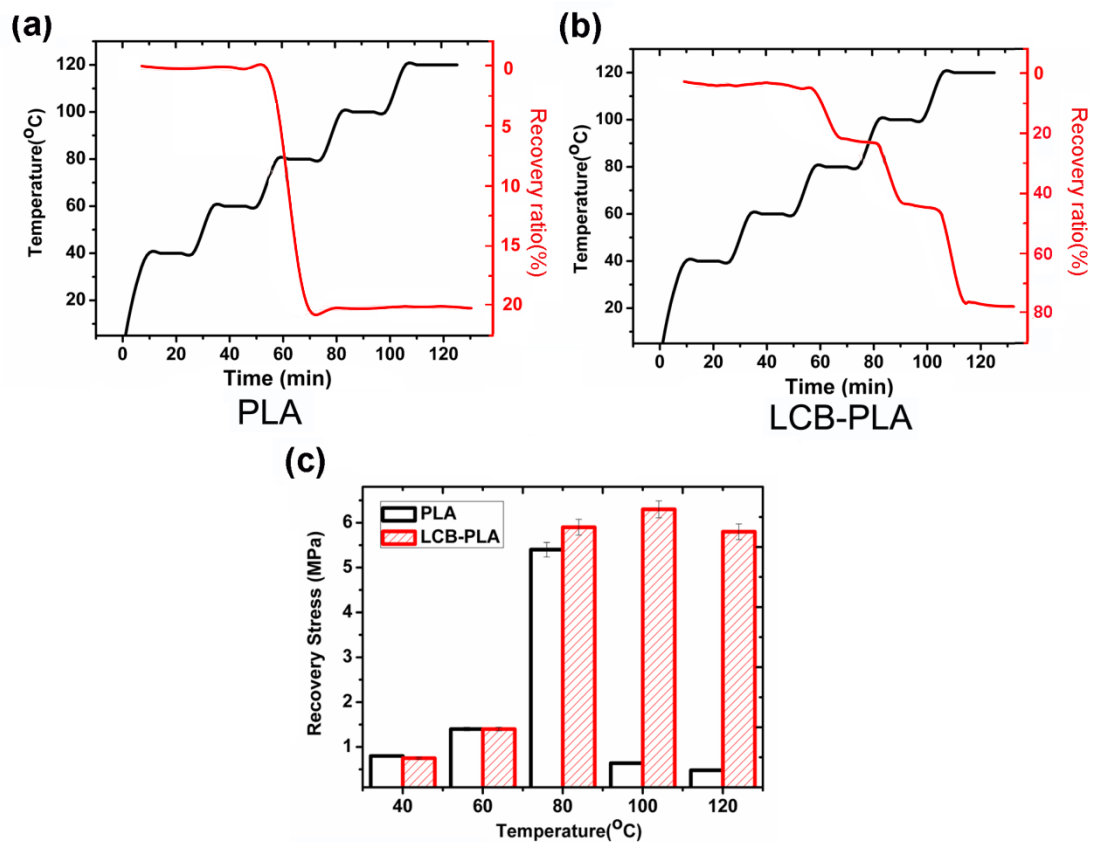

Fig. 2 DMA curves of oriented (a) PLA and (b) LCB-PLA during shape recovery process; (c) Recovery stress of oriented PLA and LCB-PLA

**Shape memory behavior of oriented PLA and LCB-PLA at different stage of solid-phase die drawing process**

As shown in Fig.3, in the orientation process of solid die drawing, PLA sample was made up of three distinct zones: undeformed part (Region I), the part which deformed within the die (Region Π) and the part drawn out of the die where a substantial free drawing can occur (Region Ⅲ). The shape recovery behavior of all oriented samples at two portions along the drawing direction was investigated as shown in Fig. 3: the sample at Portion B in Region Π, which was just drawn out of the die exit, underwent only die drawing; the sample at Portion C in Region Ⅲ underwent both die drawing and free drawing.
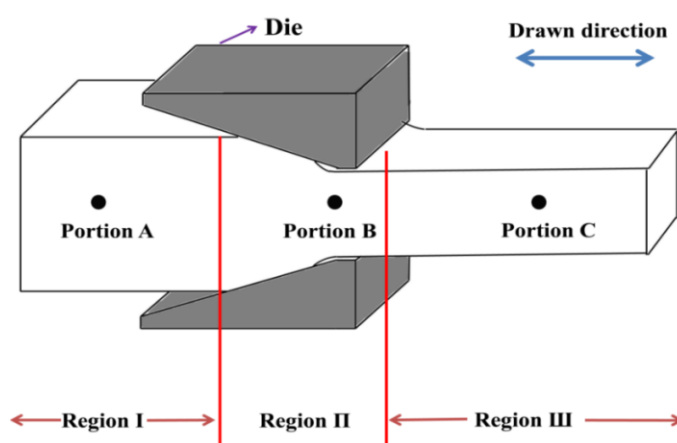
Fig. 3 Three distinct zones of PLA samples during die drawing

The 2D-WAXD patterns at these two portions for PLA and LCB-PLA samples after orientation and recovery were shown in Fig.4. For the oriented samples before recovery, two strong circular spots on the equator of (200)/(110) reflection and a four-point image of (203) reflection can be observed demonstrating that PLA chains oriented along the drawing direction. For samples after being recovered under 60°C, the patterns kept almost unchanged compared with the samples before recovery. When the temperature increased to 80~120 $^{\circ}$C, the four-point image of (203) reflection of PLA and LCB-PLA samples disappeared gradually, suggesting the obvious recovery

9
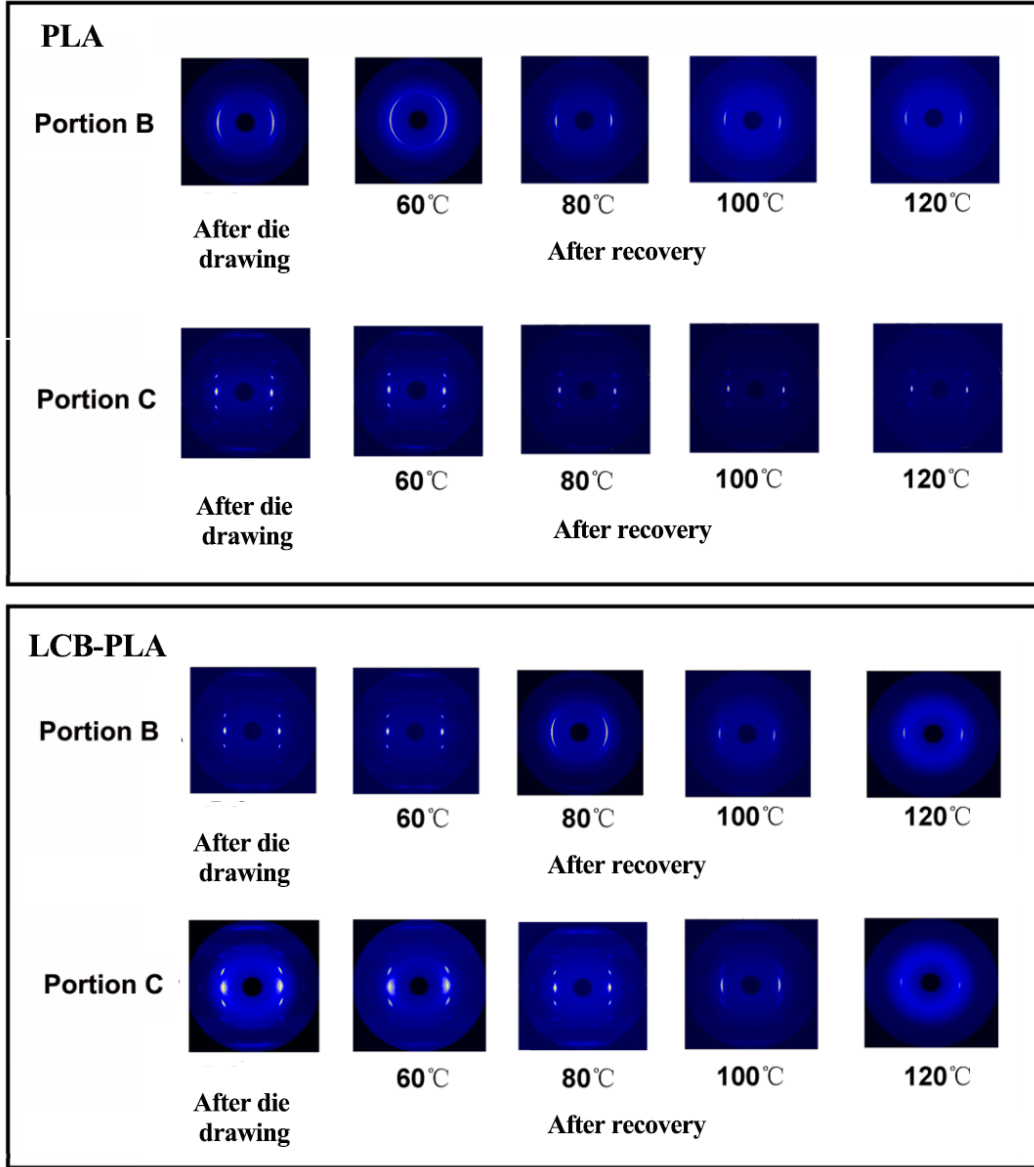
of samples.

Fig. 4 2D-WAXD patterns of oriented PLA and LCB-PLA samples after orientation and recovery

The orientation factors (F) of PLA samples can be calculated as follows [21]:

$$F = \frac{3\langle\cos^2\emptyset\rangle - 1}{2} \tag{3}$$

$$\langle\cos^2\emptyset\rangle = \frac{\int_0^{\pi/2} I(\emptyset)\sin\emptyset\cos^2\emptyset d\emptyset}{\int_0^{\pi/2} I(\emptyset)\sin\emptyset d\emptyset} \tag{4}$$

where $I(\Phi)$ was the scattering intensity along the angle Φ.

Moreover, F_{die}, the orientation factor of the sample just suffering die drawing, can

be determined by the sample located at Portion B, while F_{final}, the orientation factor of

the final sample, can be determined by the sample located at Portion C, and thus, F_{free}, the orientation factor of the sample just suffering free drawing outside the die, can be calculated as:

$$F_{free} = F_{final} - F_{die} \qquad (5)$$

Then, the recovery of orientation degree (R_{OD}) can be calculated as:

$$R_{OD\text{-}final} = （F_{final} - F_{rec\text{-}final}） / F_{final} \cdot 100\% \qquad (6)$$

$$R_{OD\text{-}die} = （F_{die} - F_{rec\text{-}die}） / F_{die} \cdot 100\% \qquad (7)$$

$$R_{OD\text{-}free} = （F_{free} - F_{rec\text{-}free}） / F_{free} \cdot 100\% \qquad (8)$$

where, F_{final}, F_{die} and F_{free} were the orientation factor of the final oriented sample, sample just suffering die drawing and sample just suffering free drawing before recovery, respectively; $F_{rec\text{-}final}$, $F_{rec\text{-}die}$ and $F_{rec\text{-}free}$ were the orientation factor of the final oriented samples, sample just suffering die drawing and sample just suffering free drawing after recovery.

As shown in Fig.5, the contribution of die drawing and free drawing to the R_{OD} of PLA samples at different recovery temperatures was discriminated. At Portion C where the final oriented samples were produced, the $R_{OD\text{-}final}$ of PLA samples showed the trend of increasing at first and then keeping stable with the increase of recovery temperature. For LCB-PLA samples, the $R_{OD\text{-}final}$ increased continuously in the whole temperature range, and moreover, when the temperature was higher than 80°C, $R_{OD\text{-}final}$ increased with a very high speed. At portion B, where samples just suffered die drawing, the $R_{OD\text{-}die}$ of PLA samples increased gradually with the recovery temperature, while $R_{OD\text{-}die}$ of LCB-PLA samples increased sharply above 80°C. For samples just suffering free drawing, the $R_{OD\text{-}free}$ values of both PLA and LCB-PLA samples increased quickly at first and then kept constant. Therefore, it can be concluded that, for oriented PLA, the recovery curve of the final sample showed the

same trend with that of sample suffering just free drawing; while for oriented LCB-PLA, the recovery curve of the final sample showed the same trend with that of sample drawn just with die.
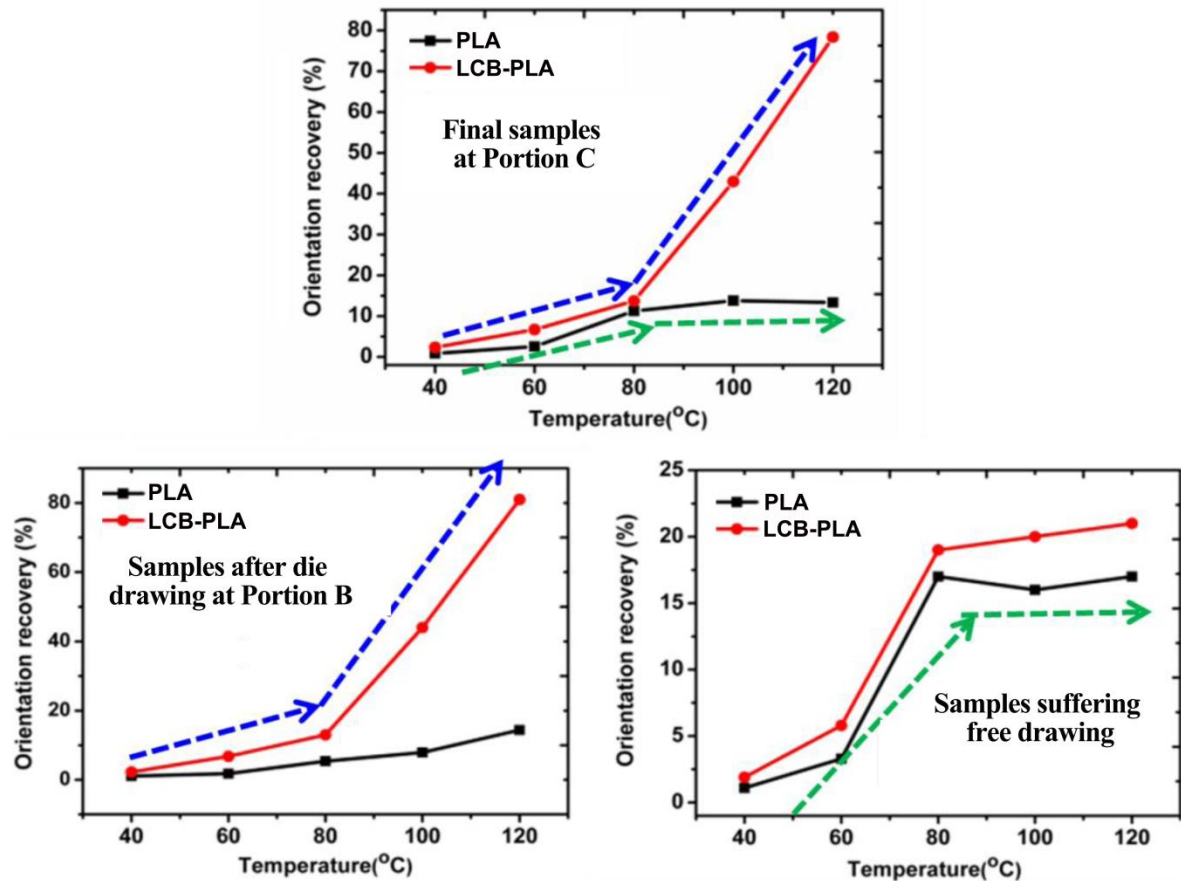
Fig. 5 The effect of die drawing process and free drawing process on the recovery ratio of oriented PLA and LCB-PLA samples

The effect of shape recovery on the mechanical properties of highly oriented PLA and LCB-PLA

After shape recovery, the mechanical properties of highly oriented PLA and LCB-PLA were shown in Fig.6. For PLA, the tensile strength and modulus decreased as the recovery temperature increased from 60 ℃ to 80 ℃ and then maintained constant with continuously increasing temperature from 80 ℃ to 120 ℃. While, for LCB-PLA, its mechanical properties were strongly dependent on the recovery temperature. When the temperature increased from 60 ℃ to 120 ℃, both the tensile strength and the modulus nearly showed a linear downward trend with the temperature.

Therefore, by regulating the recovery temperature of oriented LCB-PLA, the shape recovery ratio and mechanical strength can be effectively controlled, and thus the self-reinforced and self-fastening effect can be achieved simultaneously for PLA as bone fixation material.
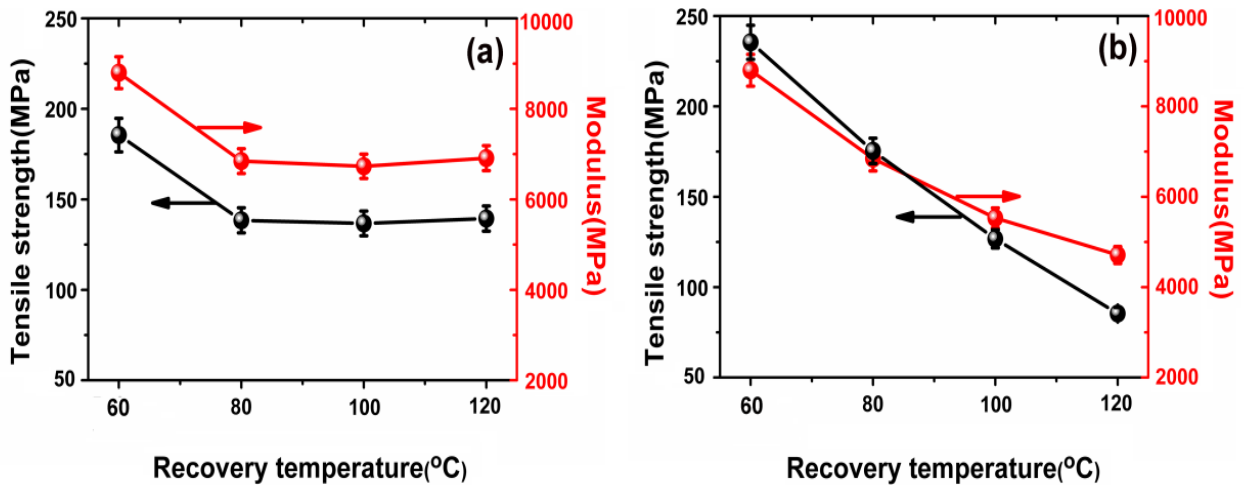

Fig. 6 Mechanical properties of PLA (a) and LCB-PLA (b) after recovery at different temperature

DISCUSSION

The different influence of die drawing and free drawing on the recovery behaviors may be attributed to the different entanglement degree and orientation structure formed during drawing process between PLA and LCB-PLA. So, in order to explore the shape recovery mechanism of highly oriented PLA samples, the structure evolution on the nanoscale for PLA and LCB-PLA during orientation process of solid die drawing and shape recovery process was studied.

For PLA, the 2D-SAXS patterns of the sample at Portion A, B and C after die drawing and shape recovery were illustrated in Fig.7. For samples at Portion A, the pattern of 2D-SAXD showed circle-like scattering profile, which was the result of the isotropic morphology, indicating the absence of any detectable orientation structures. For samples at Portion B after orientation, the 2D-SAXD pattern showed elliptical arc pattern, which suggested that supermolecular structure with less orientation (most likely oriented spherulits) existed in the sample. For samples at Portion C after

13

orientation, a strong streak pattern on the equator was observed indicating that the superstructure of the sample was mainly a fibrillar structure. After being recovered at different temperature, the 2D-SAXD patterns of the samples at Portion B changed little. While, for the pattern of samples at Portion C after recovery, the signal along the equator direction was shortened, indicating that the orientation degree of the sample was reduced and the periodicity was weakened.
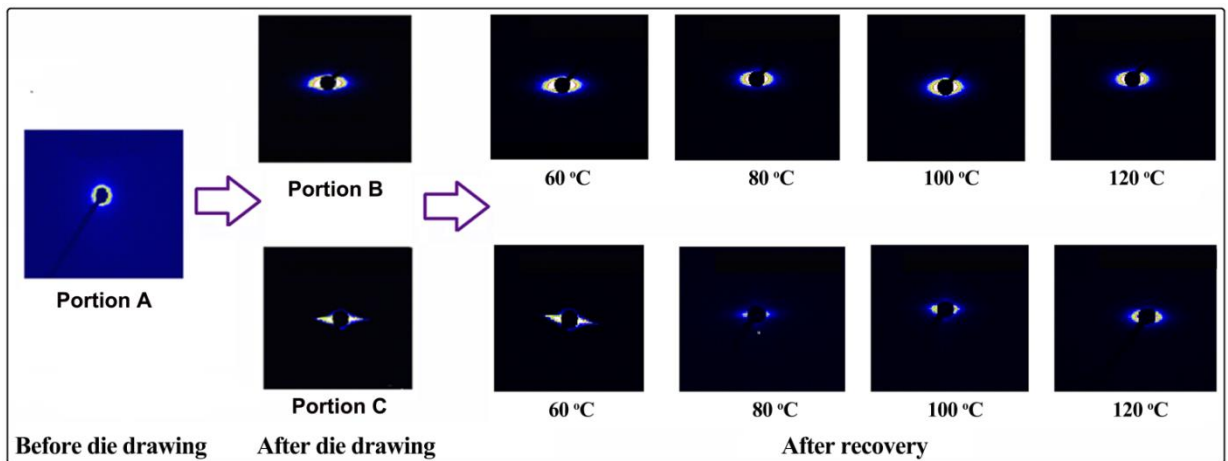

Fig. 7 2D-SAXS patterns of PLA at Portion B and Portion C during die drawing and shape recovery process

For further studying the inner structure of long period, known as being composed of the crystalline and amorphous region, more detailed information could be acquired from the electron density correlation function K(z) as follows [22]:

$$K(z)=\frac{\int_0^\infty I（q） \cos(qz)dq}{\int_0^\infty I（q） dq} \tag{9}$$

where z was the drawing direction.

The K(z) curves of PLA samples after orientation and shape recovery were shown in Fig.8(a). The position of the first peak minimum corresponded with the lamellar thickness (L_c), while the position of the first peak maximum corresponded with the long period (L_{ac}), and thus the average thickness of the amorphous layer (L_a) was then given by the relation of $L_a = L_{ac} - L_c$.

The variation of L_{ac}, L_c and L_a of PLA samples during orientation and shape

14

recovery process was shown as Fig. 8(b). During orientation process, compared with the undeformed sample at Portion A, for samples just suffering die drawing at Portion B, the L_{ac}, L_a and L_c value almost remained constant, resulting from the low orientation degree and crystallinity of PLA samples induced by the die drawing process. However, when samples were first drawn through the die and then were free drawn at Portion C, the values of L_{ac}, L_a and L_c increased.

During the shape recovery process for PLA samples at Portion B, with increasing recovery temperature from 60 ℃ to 120 ℃, the L_{ac}, L_a and L_c maintained almost constant. At Portion C, with increasing recovery temperature from 60 ℃ to 80 ℃, the L_{ac} and L_a decreased while L_c maintained constant, suggesting that the shape recovery behavior at 80 ℃ was resulted from the chain relaxation of the amorphous phase of PLA. With the further increase of recovery temperature from 80 ℃ to 120 ℃, the L_{ac}, L_a and L_c of PLA samples maintained constant.
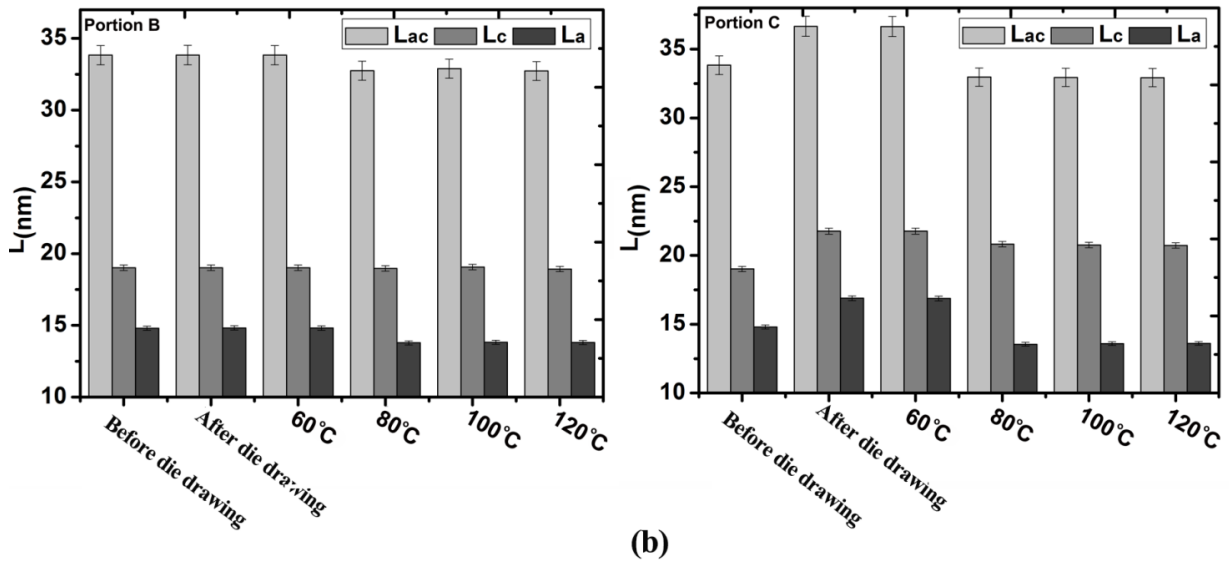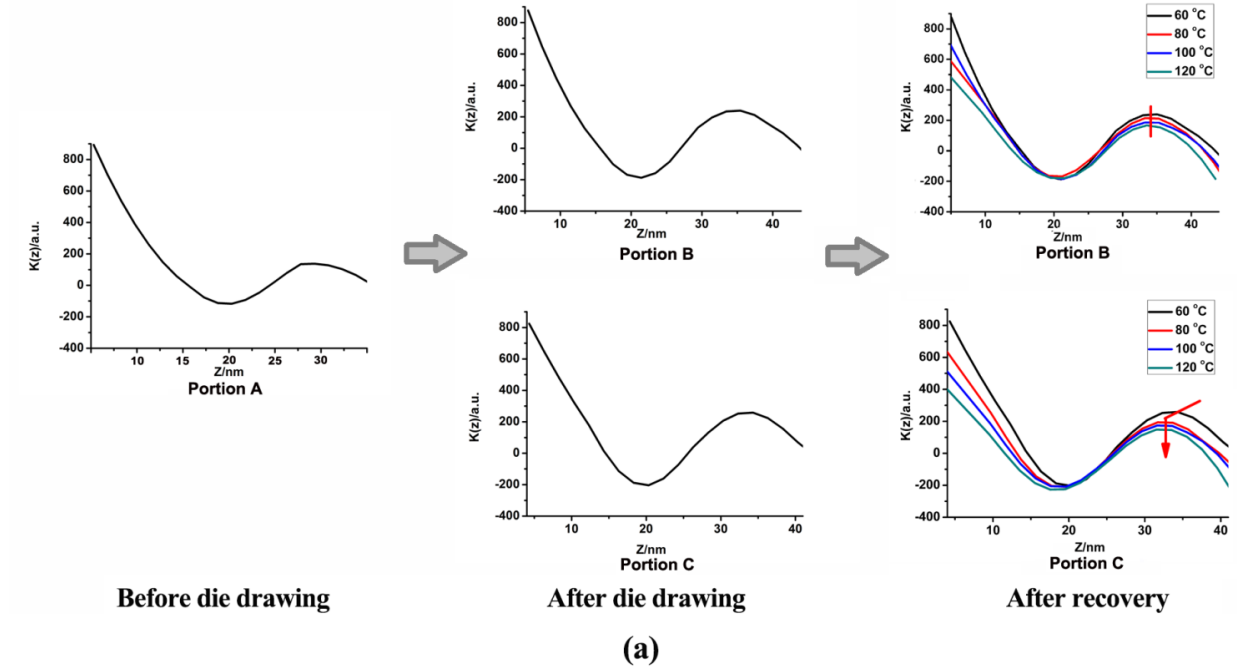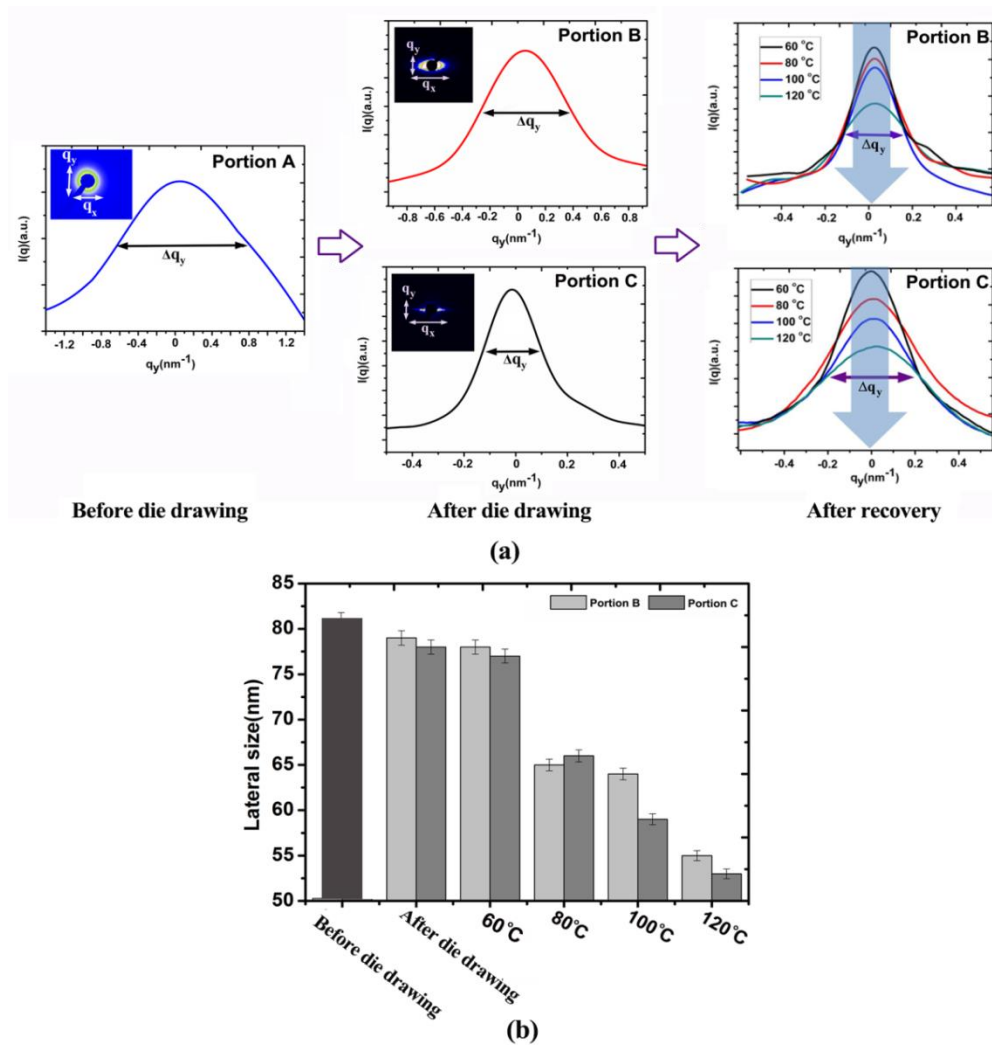
Fig. 8 K(z) curves (a) and the average value of L_{ac}, L_a, L_c (b) of PLA during die drawing and shape recovery process

As shown in Fig.9, the size of the lamellae ($L_{lateral}$) can be derived from the scattering intensity distribution ($I(q_y)$) along the q_y direction according to $L_{lateral}=2\pi/\Delta q_y$ (Δq_y was the width of the peak at half height of the curve). [23]

The average values of $L_{lateral}$ for PLA samples at Portion A, B and C during die drawing process and shape recovery process were shown in Fig.9(b). Obviously, when PLA were first drawn through the die and then was free drawing, $L_{lateral}$ decreased

gradually, indicating the formation of small lamellae due to stress-induced crystallization. During shape recovery process, at both Portion B and Portion C, with increasing recovery temperature from 60 ℃ to 120 ℃, the $L_{lateral}$ further decreased for PLA samples, indicating the chain relaxation, rearrangement and cold crystallization of amorphous phase of PLA and thus the formation of small size lamellae.


Fig. 9 The I(qy) curves (a) and the average value of $L_{lateral}$ (b) for PLA during die drawing and shape recovery process

Meanwhile, 2D-SAXS was also performed to explore the structure evolution and the shape recovery mechanism of highly oriented LCB-PLA samples. The 2D-SAXS patterns for LCB-PLA samples after die drawing and shape recovery was shown in Fig.10. It can be seen that the SAXS pattern changed from isotropic scattering ring to two-bar like on the meridian for samples after orientation both at Portion B and C,

which indicated the ''original'' lamellar stacks perpendicular to the stretching direction were destroyed to form new oriented mesomorphic phase parallel to the stretching direction with stretched-out chains conformation.

During shape recovery process, with increasing recovery temperature, the intensity of scattering patterns along the equatorial direction for LCB-PLA samples gradually decreased, which indicated that the initial deformation was reverted. Besides, with increasing recovery temperature, the two-bar SAXS pattern on the meridian gradually disappeared, which showed that the oriented mesomorphic phase was destroyed and the stretched-out chains parallel to the stretching direction relaxed and recovered. When the recovery temperature reached 120°C, streak-like scattering pattern in the meridional direction together with two sharp triangular streaks in the equatorial direction can be observed, indicating that shish-kebab crystalline structure formed.
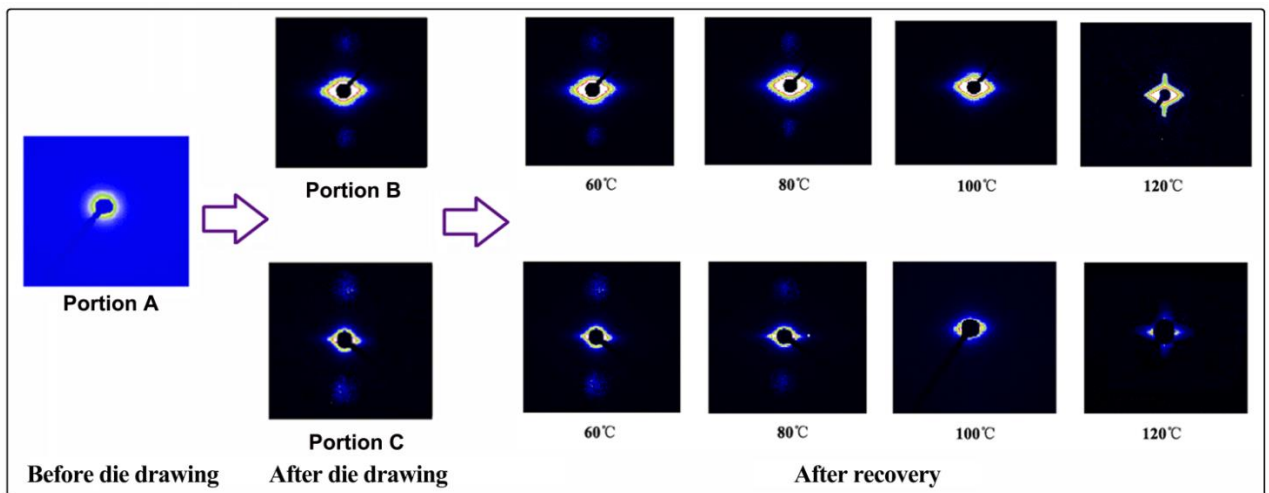
Fig. 10 2D-SAXS patterns of LCB-PLA at Portion B and Portion C during die drawing and shape recovery process

The K(z) curves of LCB-PLA samples before and after shape recovery were shown in Fig. 11(a), and the related L_{ac}, L_c and L_a were shown in Fig.11(b). During the orientation process, both for samples at Portion B and C, L_{ac}, L_a and L_c all increased. After shape recovery, with the increase of recovery temperature from 60 ℃

to 120 ℃, the L_{ac} and L_a continuously decreased, while the L_c changed slightly, suggesting the approaching of lamellae and the curling of molecular chain of both amorphous phase and oriented mesomorphic phase, which demonstrated the occurrence of successive and continuous shape recovery in the temperature range of 80℃ to 120℃.
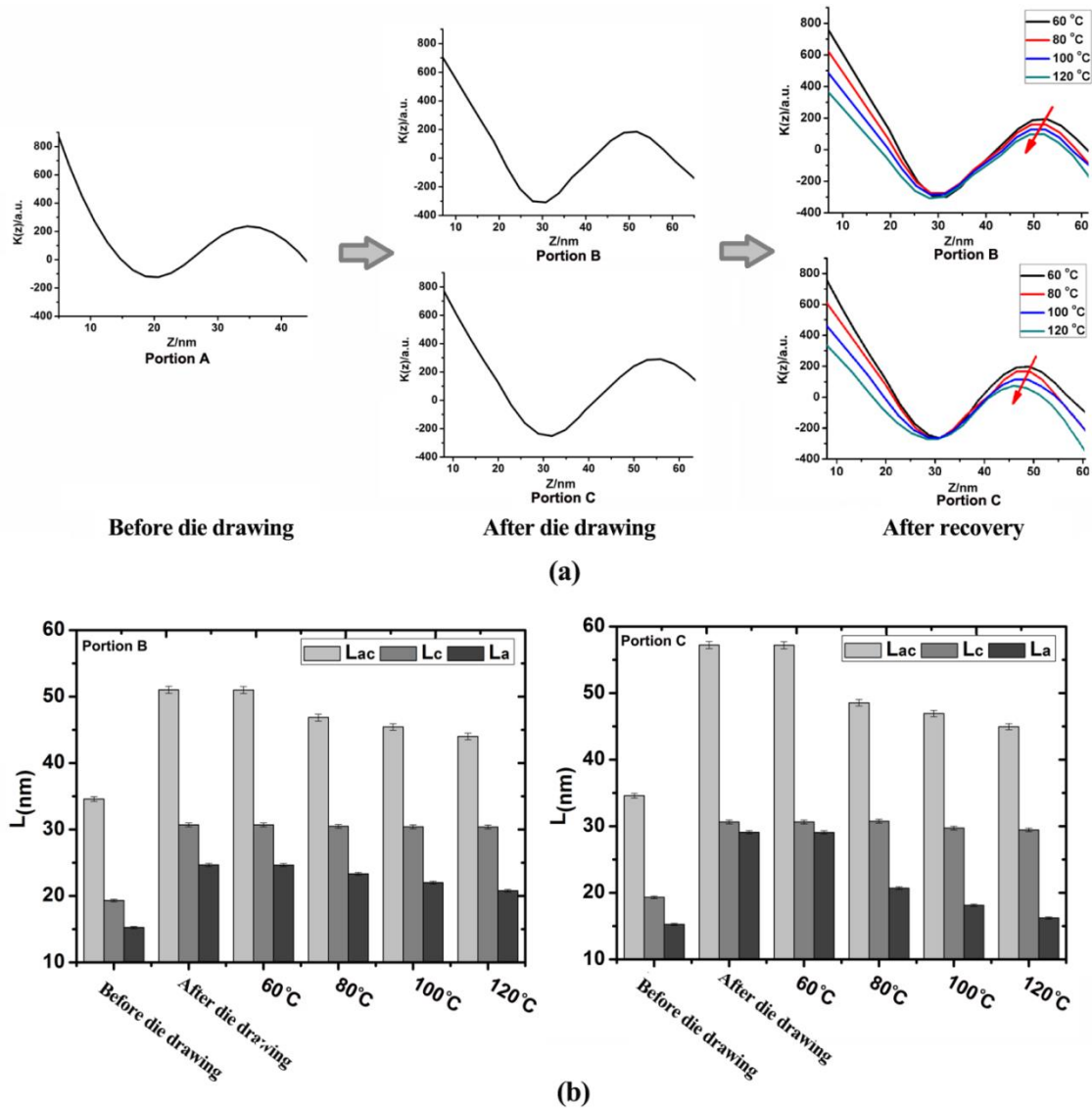
Fig. 11 K(z) curves (a) and the average value of L_{ac}, L_a, L_c (b) of LCB-PLA at Portion B and Portion C during die drawing and shape recovery process

The curves of $I(q_y)$ of LCB-PLA samples were shown in Fig.12(a), and the $L_{lateral}$ values were illustrated in Fig.12(b). As LCB-PLA samples were first drawn through the die and then free drawn, the $L_{lateral}$ decreased. The chain slipping of LCB-PLA would be restricted by its poor chain mobility, thereby fragmentation of neighboring

crystal lamella occurring. After shape recovery, as the recovery temperature changed from 60℃ to 120℃, the $L_{lateral}$ of LCB-PLA samples both at Portion B and C increased, which was attributed to the recovery of the mesomorphic phase and the formation of shish-kebab crystalline structure.
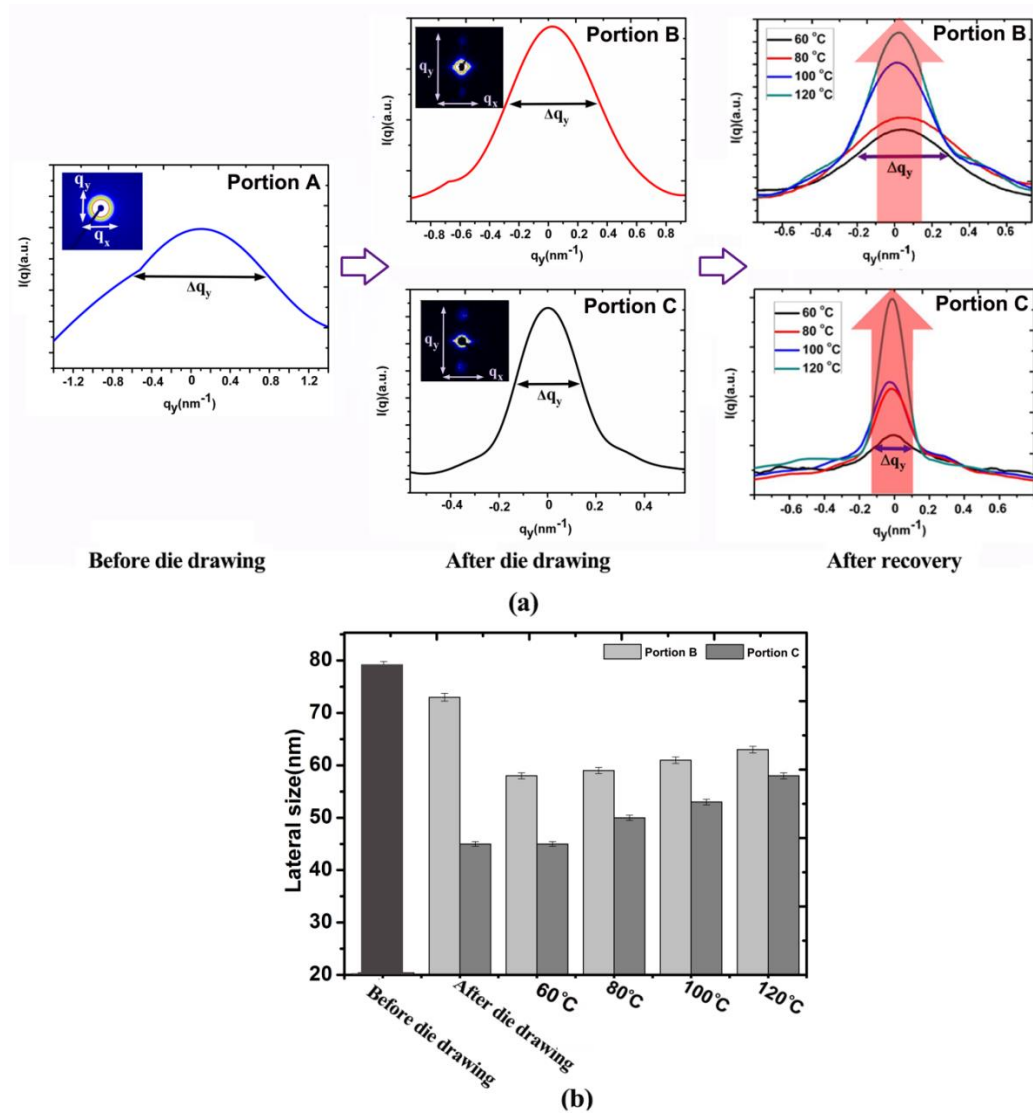
Fig. 12 The I(qy) curves （a) and the average value of $L_{lateral}$ (b) for LCB-PLA during die drawing and shape recovery process

In conclusion, the shape recovery mechanism of PLA and LCB-PLA sample was quite different. As shown in Fig.13, for PLA, when it was drawn through the converging die, shear-induced orientation and crystallization were hardly retained, while in the subsequent free stretching stage, perfect oriented lamellar structure formed. During shape recovery process, when the temperature reached 80℃ (slightly

higher than T_g of PLA), the chain segment in its amorphous phase relaxed, which triggered shape recovery of the sample, resulting in a decrease of L_{ac} and L_a. However, with further increasing temperature from 80 ℃ to 120 ℃, the relaxed chain segment of the amorphous phase cannot provide enough driving force for shape recovery, and thus the L_{ac}, L_c and L_a maintained constant.

For LCB-PLA, lots of oriented mesomorphic phase formed during orientation process of solid die drawing, which was easy to be damaged at elevated temperatures, and thus together with amorphous phase, the oriented mesomorphic phase, can act as switching domains. Upon heating, with increasing temperature from 60 ℃ to 80 ℃, the chain segment of amorphous phase relaxed, which triggered the first macroscopical shape recovery, leading to the decrease of L_{ac} and the L_a. Then, with increasing temperature from 80 ℃ to 120 ℃, the oriented mesomorphic phase gradually relaxed resulting in the subsequent multi-shape recovery, and thus the L_{ac} and L_a further decreased. Besides, the increase of $L_{lateral}$ for LCB-PLA samples was attributed to formation of shish-kebab crystalline structure.
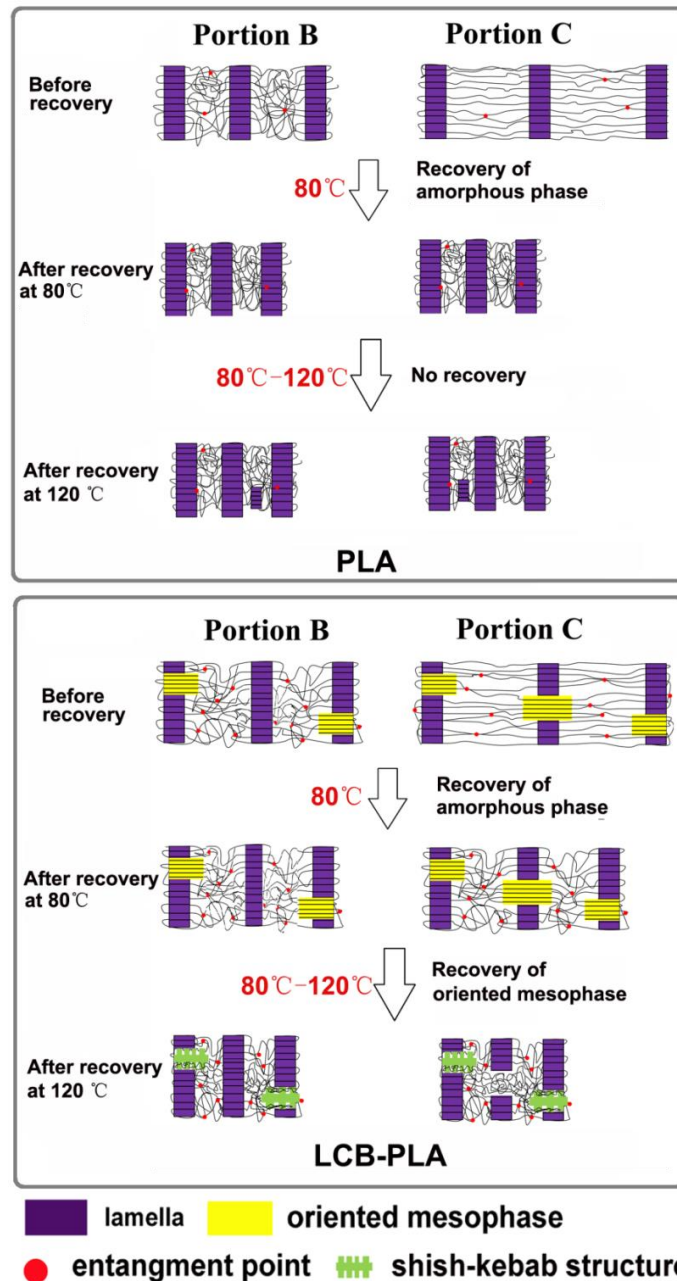
Fig. 13 Proposed morphology evolution of PLA and LCB-PLA during recovery

CONCLUSION

Highly oriented LCB-PLA was prepared through solid-phase die drawing technology and its shape memory effect was studied by comparison with PLA. For PLA, in the temperature range of 60~120 °C, only one-step recovery at 80°C with recovery ratio of 21.5% can be observed, while, for LCB-PLA, multiple recovery behavior with high recovery stress and high recovery ratio of 78.8% was achieved. For oriented PLA, the recovery curve of the final sample showed the same trend with

that of sample suffering just free drawing; while for oriented LCB-PLA, the recovery curve of the final sample showed the same trend with that of sample drawn just with die. After shape recovery, the mechanical properties of LCB-PLA showed a linear downward trend with the recovery temperature. The oriented mesomorphic phase together with the amorphous phase of LCB-PLA can act as switching domains, and upon heating, the chain segment in these domains gradually relaxed, triggering the continuous shape recovery and resulting in decreasing of L_{ac} and L_a. By regulating the recovery temperature of oriented LCB-PLA, both self- reinforced and self-fastening effects were achieved simultaneously for PLA as bone fixation material.

Acknowledgements

References

[1] Gunatillake P A, Adhikari R. Biodegradable synthetic polymers for tissue engineering. *Eur. Cell.* Mater. **2003**, 5, 1

[2] Rasal R M, Janorkar A V, Hirt D E. Poly (lactic acid) modifications. *Progress in polymer science*, **2010**, 35, 338.

[3]Lopes M S, Jardini A L, Maciel Filho R. Poly (lactic acid) production for tissue engineering applications. *Procedia Engineering*. **2012**, 42, 1402.

[4] Sharkawi, T., Darcos, V., & Vert, M. Poly (DL‑lactic acid) film surface modification with heparin for improving hemocompatibility of blood-contacting bioresorbable devices. *J. Biomed. Mater. Res. A*. **2011**, 98, 80-87.

[5] Niu, X., Luo, Y., Li, Y., Fu, C., Chen, J., Wang, Y. Design of bioinspired polymeric materials based on poly (D, L‑lactic acid) modifications towards improving its cytocompatibility. *J. Biomed. Mater. Res. A.* **2008,** 84, 908-916.

[6] Slivka, M. A.; Chu, C. C. Fiber-matrix Interface Studies on Bioabsorbable Composite Materials for Internal Fixation of Bone Fractures. II. A New Method Using Laser Scanning Confocal Microscopy. *J. Biomed. Mater. Res.*: An Official Journal of The Society for Biomaterials and The Japanese Society for Biomaterials, **1997**, 37, 353.

[7] Felfel, R. M.; Ahmed, I.; Parsons, A. J.; Haque, P.; Walker, G. S.; Rudd, C. D. Investigation of Crystallinity, Molecular Weight Change, and Mechanical Properties of PLA/PBG Bioresorbable Composites As Bone Fracture Fixation Plates. *J. Biomater. Appl.* **2012**, 26, 765.

[8] Yu, L.; Liu, H.; Xie, F.; Chen, L.; Li, X. Effect of Annealing and Orientation on Microstructures and Mechanical Properties of Polylactic Acid. *Polym. Eng. Sci.* **2008**, 48, 634.

[9] Yuan, X.; Mak, A. F.; Kwok, K. W.; Yung, B. K.; Yao, K. Effect of Annealing and Orientation on Microstructures and Mechanical Properties of Polylactic Acid. *J. Appl. Polym. Sci.* **2001**, 81, 251.

[10] Gupta, B.; Revagade, N.; Anjum, N.; Atthoff, B.; Hilborn, J. Preparation of Poly (Lactic Acid) Fiber by Dry-jet-wet-spinning. I. Influence of Draw Ratio on Fiber Properties. *J. Appl. Polym. Sci.* **2006**, 100, 1239.

[11] Li, Z.; Ye, L.; Zhao, X.; Coates, P.; Caton-Rose, F.; Martyn, M. High Orientation of Long Chain Branched Poly (Lactic Acid) with Enhanced Blood Compatibility and Bionic Structure. *J. Biomed. Mater. Res. A*. **2016**, 104, 1082.

[12] Li, J.; Li, Z.; Ye, L.; Zhao, X.; Coates, P.; Caton-Rose, F.; Martyn, M. Structure Evolution and Orientation Mechanism of Long-Chain-Branched Poly (Lactic Acid) in the Process of Solid Die Drawing. *Eur. Polym. J.* **2017**, 90, 54.

[13] Zhao X., Ye L. Structure and properties of highly oriented polyoxymethylene produced by hot stretching. *Mater. Sci. Eng. A -Struct.* **2011**, 528, 4585-4591

[14] Zhao X., Ye L. Structure and properties of highly oriented polyoxymethylene/multi-walled carbon nanotube composites produced by hot stretching, *Compos. Sci. Technol.* **2011**, 71, 1367-1372

[15] Kunpeng Ruan, Yongqiang Guo, Yusheng Tang, Yali Zhang, Jiani Zhang, Mukun He, Junwei Gu. Improved thermal conductivities in polystyrene nanocomposites by incorporating thermal reduced graphene oxide via electrospinning-hot press technique. *Compos. Commun.* **2018**, 10, 68-72.

[16] Gu, J., Lv, Z., Wu, Y., Guo, Y., Tian, L., Qiu, H., Zhang, Q. Dielectric thermally conductive boron nitride/polyimide composites with outstanding thermal stabilities via in-situ polymerization-electrospinning-hot press method. *Compos. Part A-Appl. S.* **2017**, 94, 209-216.

[17] Chokphoemphun, S., Hinthao, C., Eiamsa-ard, S., Promvonge, P., Thianpong, C. Thermal Performance in Circular Tube with Co/Counter-Twisted tapes. *Adv. Mater. Res. Trans. Tech. Publ.* **2014**, 931, 1198-1202.

[18] Xu, X., Yang, Q., Wang, Y., Yu, H., Chen, X., & Jing, X. Biodegradable electrospun poly (L-lactide) fibers containing antibacterial silver nanoparticles. *Eur. Polym. J.* **2006**, 42, 2081-2087.

[19] Jeong, S. I., Lee, A. Y., Lee, Y. M., Shin, H. Electrospun gelatin/poly (L-lactide-co-ε-caprolactone) nanofibers for mechanically functional tissue-engineering scaffolds. *J Biomat. Sci.-Polym. E.* **2008**, 19, 339-357.

[20] Zhang, F., Zhang, Z., Liu, Y., & Leng, J. Shape memory properties of electrospun Nafion nanofibers. *Fiber. Polym.* **2014**, 15, 534-539.

[21] Jin, M.; Liu, K.; Liu, H.; Zhang, Y.; Du, H.; Li, X.; Zhang, J. Effects of Polyolefin Elastomer and B-Nucleating Agent on Morphological Evolution of Isotactic Polypropylene under An Intensive Shear Rate. *Polym. Test.* **2014**, 39, 1.

[22] Rotella, C.; Tencé-Girault, S.; Cloitre, M.; Leibler, L. Shear-Induced Orientation of Cocontinuous Nanostructured Polymer Blends. *Macromolecules*, **2014**, 47, 4805.

[23] Liu, G.; Zheng, L.; Zhang, X.; Li, C.; Wang, D. Critical Stress for Crystal Transition in Poly (Butylene Succinate)-Based Crystalline–Amorphous Multiblock Copolymers. *Macromolecules*, **2014**, 47, 7533.

Figure captions

Fig. 1 Photos of shape recovery process for oriented PLA and LCB-PLA after recovery at different temperature

Fig. 2 DMA curves of oriented (a) PLA and (b) LCB-PLA during shape recovery process; (c) Recovery stress of oriented PLA and LCB-PLA

Fig. 3 Three distinct zones of PLA samples during die drawing

Fig. 4 2D-WAXD patterns of oriented PLA and LCB-PLA samples after die drawing and recovery

Fig. 5 The effect of die drawing process and free drawing process on the recovery ratio of oriented PLA and LCB-PLA samples

Fig. 6 Mechanical properties of PLA (a) and LCB-PLA (b) after recovery at different temperature

Fig.7 2D-SAXS patterns of PLA at Portion B and Portion C during die drawing and shape recovery process

Fig. 8 K(z) curves (a) and the average value of L_{ac}, L_a, L_c (b) of PLA during die drawing and shape recovery process

Fig. 9 The I(qy) curves   (a) and the average value of $L_{lateral}$ (b) for PLA during die drawing and shape recovery process

Fig. 10 2D-SAXS patterns of LCB-PLA at Portion B and Portion C during die drawing and shape recovery process

Fig. 11 K(z) curves (a) and the average value of L_{ac}, L_a, L_c (b) of LCB-PLA at Portion B and Portion C during die drawing and shape recovery process

Fig. 12 The I(qy) curves   (a) and the average value of $L_{lateral}$ (b) for LCB-PLA during die drawing and shape recovery process

Fig. 13 Proposed morphology evolution of PLA and LCB-PLA during recovery

Table of Contents (TOC)

Before die drawing   After die drawing   60~120°C   After recovery

Mesomorphic phase formed.   Mesomorphic phase relaxed and shish-kebab crystalline structure formed.